OPTIMIZED AIR-TO-REFRIGERANT HEAT EXCHANGER WITH LOW-GWP REFRIGERANTS

Honghuyun Cho[(a)], Piotr A. Domanski[(b)]
[(a)]Chosun University
Gwangju, 501-753, S. Korea, hhcho@chosun.ac.kr
[(b)]National Institute of Standards and Technology
Gaithersburg, MD 20899-8631, USA, piotr.domanski@nist.gov

ABSTRACT

This paper presents an analytical evaluation of the performance of low-GWP refrigerants in a finned-tube evaporator used for residential cooling applications. The study employed an evolutionary-computation optimization module to examine the effect of a refrigerant circuitry design on performance of twelve alternative refrigerants for R22 and R410A. The study showed that high-pressure fluids benefited most from refrigerant circuitry optimization, with R744 achieving a capacity increase of over 13 %. Among lower-pressure fluids, the capacity of an R717 evaporator increased by over 10 %. The effect of optimized refrigerant circuitries on the system performance was estimated. The results show that zeotropic blends with a large temperature glide are particularly sensitive to the refrigerant circuitry and may suffer significant performance degradation in heat exchangers with improper design.

Keywords: air conditioning, evaporator, global warming potential, optimization, refrigerants

1. INTRODUCTION

Concerns about climate change, and the recent (EU, 2014) and anticipated regulations phasing down refrigerants with a high global warming potential (GWP), have prompted numerous studies evaluating the performance of low-GWP refrigerants in air-conditioning and refrigeration equipment. Initial performance evaluations typically rely on simple theoretical simulations, which are based on thermodynamic properties alone. The next step often involves laboratory tests in a system that was originally developed for the refrigerant planned to be phased out. While laboratory tests provide the 'most trusted' information about performance of a refrigerant in a given system, it is recognized that tests of a new refrigerant in a system optimized for a different refrigerant (referred to as 'drop-in' tests) do not show the performance potential of the new fluid. 'Soft-optimization', which includes adjustment of the refrigerant charge and expansion device, is typically implemented in drop-in tests; however, optimization of the compressor and refrigerant circuitry in the evaporator and condenser is also needed for fair refrigerant evaluation (Abdelaziz et al., 2015). In this paper we discuss the effect of refrigerant circuitry on the evaporator performance with natural and fluorinated alternatives for R22 and R410A. We applied an evolutionary computation-based optimization module to design refrigerant circuitries for candidate refrigerants and compared the optimized performance in the evaporator with that using the original circuitry.

2. REFRIGERANTS

We considered six R22 alternatives and six R410A alternatives (Table 1). We assigned the alternatives to these two groups based on the pressure of these refrigerants while operating in an air conditioner. The 'R22 group' includes three single-component fluids, R290 (propane), R1270 (propylene), and R717 (ammonia), which have very small GWPs but require

engineering measures to address application restrictions related to their A3, A3 and B2 safety classifications, respectively (ASHRAE, 2013). The other fluids are zeotropic mixtures designed to approximate R22 thermodynamic performance. One blend has the A1 safety designation, and the other two are mildly flammable (A2L). These blends present fewer safety-related application difficulties than R290, R1270, and R717; however, their GWPs are higher. The 'R410A group' includes two single-component fluids, R32 and R744 (carbon dioxide), which is the only non-flammable fluid. The other fluids are blends (all A2L). Generally, R744 and R717 are not considered to be direct replacement fluids. R744 has significantly higher pressure than other fluids and R717 can't be used with copper tubes and has high toxicity, but they are included here to elucidate issues of refrigerant circuitry optimization.

Table 1. Studied Alternative Low-GWP Refrigerants

(a) R22 alternative refrigerants

Refrigerant	Composition	Mass fraction (%)	Temperature glide[(1)] (K)	Safety classification[(2)]	GWP[(3)]
R22 (base)	R22	100	0	A1	1760
MIX-1[(4)]	R32/R125/R134a/R1234yf	13/13/31/43	4.0	A1	904
R444B	R32/R152a/R1234ze(E)	41.5/10/48.5	7.9	A2L	295
R454C	R32/R1234yf	21.5/78.5	6.1	A2L	146
R290	R290	100	0	A3	9
R1270	R1270	100	0	A3	1
R717	R717	100	0	B2	<1

(b) R410A alternative refrigerants

Refrigerant	Composition	Mass fraction (%)	Temperature glide[(1)] (K)	Safety classification[(2)]	GWP[(3)]
R410A(base)	R32/R125	50/50	0.1	A1	1924
MIX-2[(5)]	R32/R1234yf/R1234ze(E)	68/26/6	1.7	A2L	677
R32	R32	100	0	A2L	676
MIX-3[(6)]	R32/134a/1234ze(E)	76/6/18	2.7	A2L	593
R452B	R32/R125/R1234yf	67/7/26	1.0	A2L	572
R447A	R32/R125/R1234ze(E)	68/3.5/28.5	3.8	A2L	461
R744	R744	100	0	A1	1

[(1)] For isobaric evaporation at 7.2 °C dew-point temperature and inlet quality per Table 3; [(2)]ASHRAE (2013);
[(3)] Myhre at al. (2013) [(4), (5), (6)] Developmental names: N-20B, ARM-71A, HPR-2A, respectively

It is worthwhile to note the important parameters with regard to circuitry optimization. High liquid thermal conductivity improves the heat transfer, which reduces heat transfer irreversibilities. Low viscosity results in low pressure drop, and low drop in saturation temperature (T_{sat}) in relation to drop in pressure (P), dT_{sat}/dP, which allows for a high refrigerant mass flux to maximize the heat transfer while maintaining acceptable pressure drop. Other favorable characteristics are high heat of evaporation and high gas density. Figures 1 and 2 present properties for the studied refrigerants relative to the corresponding properties of R22 and R410A, respectively. The vapor specific volumes of R290, R1270 and R717 are much greater than that of R22, while their viscosities are lower. R717 has significantly greater liquid conductivity and heat of evaporation than R22. Other refrigerants have properties similar to those of R22. In case of 'R410A group', all alternatives except R744 have a higher specific vapor volume and liquid conductivity than R410A. R32 has the highest liquid conductivity among the alternatives. R744 has much lower vapor specific volume and liquid viscosity compared to all fluids including R410A.

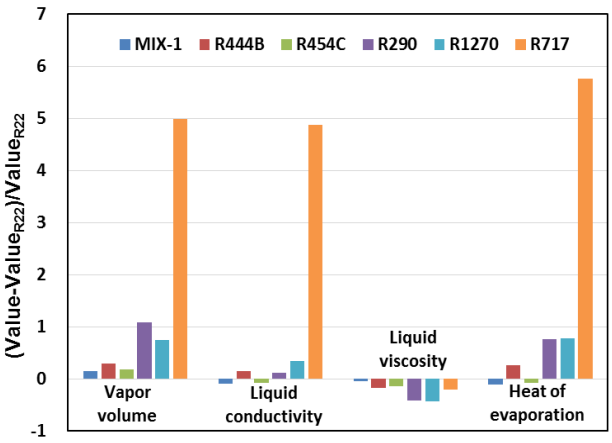

Figure 1. Vapor specific volume, liquid thermal conductivity, liquid viscosity, and heat of evaporation of R22 alternatives at 7.2 °C saturation temperature referenced to R22 properties

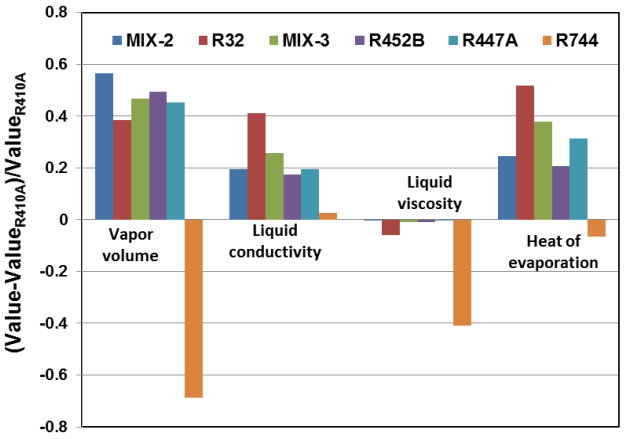

Figure 2. Vapor specific volume, liquid thermal conductivity, liquid viscosity, and heat of evaporation of R410A alternatives at 7.2 °C saturation temperature referenced to R410A properties

3. HEAT EXCHANGER SPECIFICATIONS

Figure 3 shows a schematic of the side view of the 60-tube heat exchanger as it is displayed by the graphical user interface of EVAP-COND, a public-domain design tool for finned-tube evaporators and condensers (Domanski et al., 2014). The circles represent the tubes, the solid lines denote return bends on the near side, and the broken lines denote return bends on the far side. The shown refrigerant circuitry is that of the original design with three inlets (tubes 1, 21, and 41) and three outlets (tubes 20, 40, and 60). This 3-circuit (3-pass) circuitry provides some level of robustness against a non-uniform inlet air distribution because each circuits extends through the whole width of the slab from the left-hand side to the right-hand side.

The shown heat exchanger was one of two identical slabs of a residential air conditioner's "A-shape" evaporator for which Yashar and Domanski (2009) measured the inlet air velocity using the particle image velocimetry method. The velocity profile (Figure 3) reflects the geometry of the "A-shape" assembly and the location of the condensate collection pan. The pan obstructs the airflow on the left-hand side of the coil, affecting heat transfer in tubes 1, 2 and 3 in the first depth row and another 6 tubes in the second and third row. We used this coil (including the inlet air velocity profile) in our study and optimized refrigerant circuitry (number of parallel circuits and tube connections) for each refrigerant. Table 2 provides the evaporator design information.

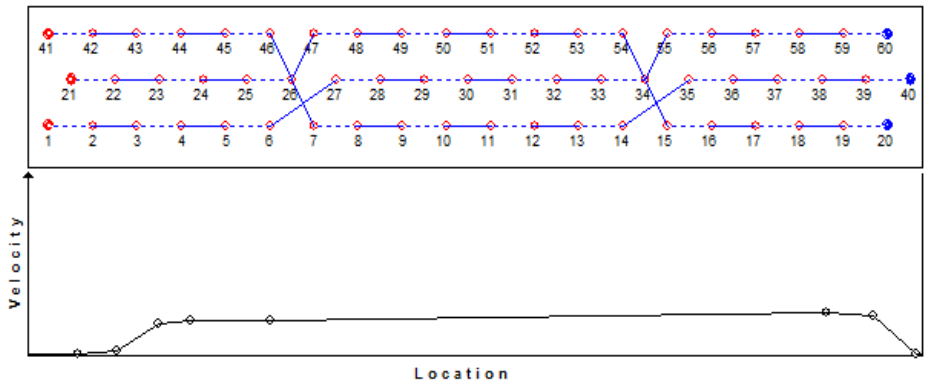

Figure 3. Side view schematic of evaporator with original tube connections and inlet air velocity profile

Table 2. Evaporator design information

Items	Unit	Value
Number of depth rows	-	3
Number of tubes per row	-	20
Tube length	mm	457
Tube pitch	mm	25.4
Tube depth row pitch	mm	19
Tube inside diameter	mm	8.7
Tube outside diameter	mm	9.5
Fin thickness	mm	0.2
Fin pitch	mm	2
Tube inner surface	-	smooth
Fin geometry	-	wavy
Tube material	-	copper
Fin material	-	aluminum
Volume flow rate of air	$m^3 s^{-1}$	0.25

Table 3. Refrigerant inlet quality

Refrigerant	Inlet quality
R22	0.176
MIX-1	0.222
R444B	0.187
R454C	0.224
R290	0.208
R1270	0.203
R717	0.108
R410A	0.220
MIX-2	0.193
R32	0.176
MIX-3	0.181
R452B	0.197
R447A	0.186
R744	0.284

4. REFRIGERANT CIRCUITRY OPTIMIZATION

4.1 Optimization Tool

We performed circuitry optimizations using the EVAP-COND package (Domanski et al., 2014). It contains first-principle-based simulation models for a finned-tube evaporator and condenser, EVAP and COND, and Intelligent System for Heat Exchanger design, ISHED. The "tube-by-tube" heat exchanger modeling scheme allows for specifying complex refrigerant circuits, modeling refrigerant distribution between these circuits, and accounting for non-uniform air distribution. Representation of refrigerant thermophysical properties is based on Lemmon et al. (2013). EVAP-COND has been validated against various experimental data sets (e.g., Payne and Domanski, 2003).

The refrigerant circuitry optimization module ISHED applies a novel methodology of *guided evolutionary computation*, which integrates methods of machine learning and evolutionary computation to assist designers in maximizing the capacity (Domanski, 2014). During the optimization run, ISHED operates on one generation (population) of circuitry architectures at a time. Each member of the population is evaluated by the heat exchanger simulator (EVAP in this study), which provides the heat exchanger's capacity as a single numerical fitness value. The designs and their fitness values are returned to ISHED's Control Module as an input for deriving the next generation of circuitry designs. This process continues for a number of iterations (generations) set by the user. After the specified number of iterations is performed, ISHED terminates the execution and reports on the best designs it has generated. In this work we set ISHED for 300 populations of 40 members; hence, 12 000 refrigerant circuitry architectures were evaluated during a single optimization run. More information on application of ISHED is presented in Domanski et al. (2005), Domanski and Yashar (2006), and Yashar et al. (2015), which includes a laboratory validation of the optimization process.

4.2 Operating Conditions Used for Optimization Runs

The following were evaporator operational parameters during the optimization runs:

- Inlet air condition: 26.6 °C dry-bulb temperature, 50 % relative humidity, 101.325 kPa pressure
- Volumetric airflow rate: 0.25 $m^3 s^{-1}$
- Refrigerant quality at the evaporator inlet: as shown in Table 3
- Refrigerant saturation temperature at the evaporator exit: 7.2 °C
- Refrigerant superheat at the evaporator exit: 5.6 °C

The refrigerant inlet quality (Table 3) was established from a vapor compression cycle in which the refrigerant undergoes the isenthalpic expansion process from 42.0 °C saturation temperature with 5.0 °C subcooling to the evaporator pressure corresponding to 7.2 °C dew-point temperature and 2.0 °C saturation temperature drop between the evaporator inlet and exit. The exception was R744 for which a transcritical cycle was used with 36.0 °C gas cooler exit temperature, 80 % effective internal heat exchanger, evaporator exit dew point of 7.2 °C with a pressure drop corresponding to 1.0 °C drop in saturation temperature. It is recognized that in an actual system with optimized compressor size and condenser circuitry, the refrigerant dew-point temperature at the evaporator exit will vary between different refrigerants; however, the use of one value (7.2 °C) is adequate because small variations in the exit dew-point temperature are not expected to change the outcome of the refrigerant circuitry optimization process.

5. OPTIMIZATION RESULTS

5.1 Performance with Refrigerant Circuitries Optimized for R22 and R410A

The symmetric layout of the original circuitry with three circuits extending through the whole width of the coil provides some level of robustness for operation with non-uniform air distribution. Nevertheless, as a preliminary step, we explored the benefit of optimization that included the measured non-uniform air distribution (Figure 3). We optimized the circuitries for R22 and R410A and then applied these optimized circuitries to other fluids. This task yielded mixed results. Figures 4 and 5 present changes in capacity (difference between capacity with the optimized circuitry for R22 or R410A, $Q_{OPT,R22}$ or $Q_{OPT,R410A}$, and the capacity of the refrigerant attained with the original circuitry Q_{ORG}, referenced to Q_{ORG}). The capacity of R22 improved by 1.9 %. Among other fluids from the 'R22 group', R290, R1270, and R717 (single-component fluids) benefited between from 2 to 3.5 times as much as R22; however, performance of zeotropic blends deteriorated. For the higher-pressure 'R410A group', capacities of all refrigerants improved by over 6 %. The lowest gain is shown for R447A, which has the highest two-phase temperature glide in this group. This task emphasized the challenge and need for optimizing refrigerant circuitries for zeotropic mixtures.

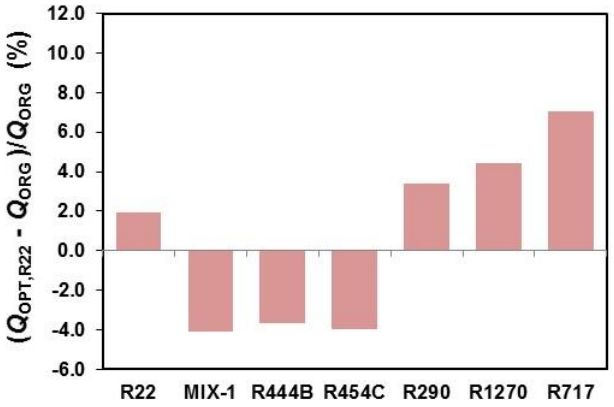

Figure 4. Capacity change for R22 and R22 alternatives with refrigerant circuitry optimized for R22 referenced to the capacity obtained by this refrigerant with the original circuitry

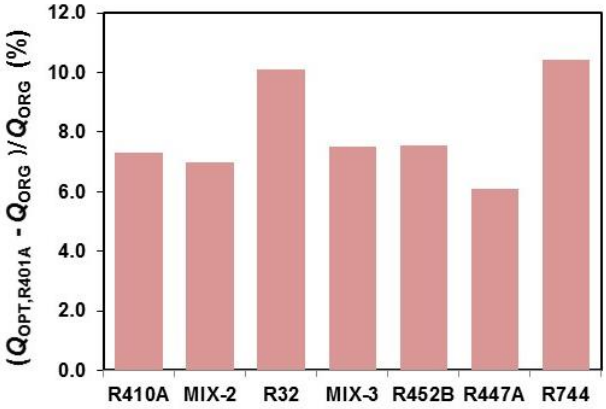

Figure 5. Capacity change for R410A and R410A alternatives with refrigerant circuitry optimized for R410A referenced to the capacity obtained by this refrigerant with the original circuitry

5.2 Performance with Refrigerant Circuitries Optimized for Each Refrigerants

With the aid of ISHED, we developed optimized circuitries for each refrigerant. As expected, each refrigerant benefited from the optimized circuitry (Figures 6 and 7). On average, the 'R410A group' (high-pressure refrigerants) benefited more from the optimization than the 'R22

group', and R22 benefited the least. These results may be related to the fact that the studied evaporator was originally designed as a component of an R22 residential air conditioner and was already optimized for R22 using traditional optimization methods. The R22 improvement may be related to ability of the ISHED-optimized design to accommodate the minimal airflow for tubes 1, 2, 3 in the first depth row and their counterparts in the second and third depth row. Examining individual fluids, capacity increases of R744 and R32 were the largest, above 12 %. In the lower-pressure 'R22 group' the largest capacity gain is shown for ammonia, above 10 %. All these fluids have outstanding thermodynamic and transport properties.

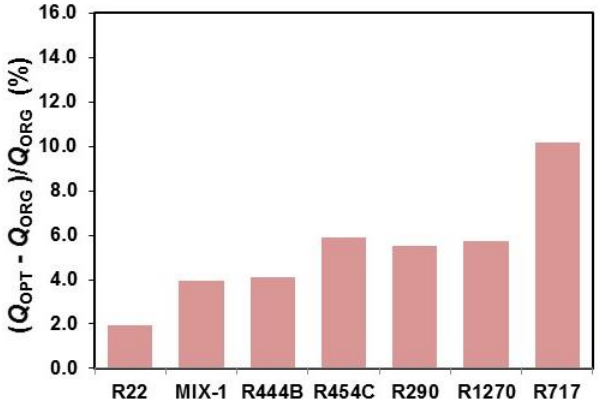

Figure 6. Capacity improvement for R22 and R22 alternatives with refrigerant circuitry optimized for each individual refrigerant referenced to the capacity obtained by this fluid with the original circuitry

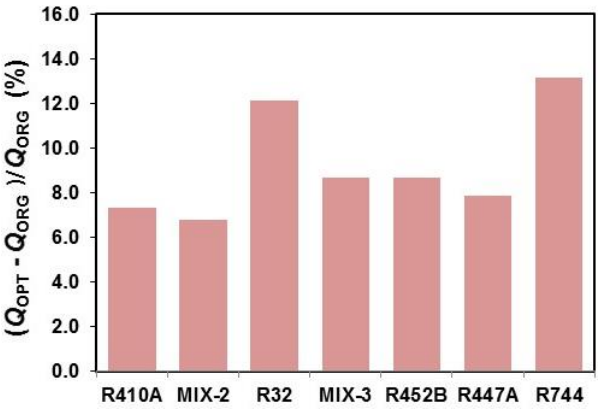

Figure 7. Capacity improvement for R410A and R410A alternatives with refrigerant circuitry optimized for each fluid referenced to the capacity obtained by this fluid with original circuitry

Table 4 presents the number of inlet and outlet tubes in the circuitries optimized for each refrigerant. For the 'R410A group', five out of seven refrigerants have one inlet tube and two outlet tubes. The highest-pressure refrigerant in the group, R744, has just one refrigerant pass, and R447A has two inlets and three outlets. The 'R22 group' (the lower-pressure group) has only R1270 in the one-inlet/two-outlets category, three refrigerants with two inlets and two outlets, R454C with two inlets and three outlets, and MIX-1 and R717 with the least restrictive circuitry using two inlets and four outlets. In general, circuitries for lower-pressure refrigerants have more parallel passes and are less restrictive to avoid excessive pressure drop and the associated drop in saturation temperature. Higher-pressure refrigerants exhibit a smaller drop of saturation temperature for a given pressure drop; this allows them to use more restrictive circuitries, which results in higher refrigerant mass fluxes and enhanced heat transfer at acceptable penalty of the saturation temperature drop. In an initially perplexing case of the least restrictive circuitry assigned for R717, reducing R717 heat transfer resistance through increasing mass flux is not beneficial because R717 heat transfer resistance is small due the outstanding thermal conductivity (particularly that of liquid), which makes the dominant share of heat transfer resistance on the air side. In this case, the penalty of the saturation temperature drop of R717 becomes the more influential factor than heat transfer improvement.

Table 4. Number of inlet and outlet tubes in ISHED-optimized circuitries[(a)]

		Number of outlet tubes			
		1	2	3	4
Number of inlet tubes	1	**R744**	**R410A, MIX-2, R32, R452B, MIX-3,** R1270		
	2		R22, R444B, R290	**R447A,** R454C	MIX-1, R717

[(a)] Bold font denotes the 'R410A group'; normal font denotes the 'R22 group'

We should note that the level of changes in evaporator capacity obtained through optimization at the same dew-point temperature at the evaporator exit will not be achieved in the actual system because the system rebalances itself at a different evaporator dew-point temperature once an evaporator of different capacity is installed. But, the results presented in Figures 6 and 7 let us estimate the system capacity and COP changes by using a simplified rating procedure for so called 'mixed systems' (Domanski, 1989). This simplified procedure applies an exponent of 0.35 and 0.21 to the evaporator capacity ratio (new evaporator over old evaporator) to estimate a change in system capacity and COP. Following this procedure, a 10 % improvement in capacity results in 3.4 % ($1.1^{0.35}$) and 2.0 % ($1.1^{0.21}$) improvement in system capacity and COP, respectively, over the values in the system with the original evaporator. For the data presented in Figure 6 and 7, the system measurements from 'drop in' tests could be better by 1 % to 4 % for the capacity and 1 % to 2.5 % for the COP. We need to emphasize the speculative nature of this assessment since the possible improvement depends on the design of the original evaporator and thermophysical characteristics of a new fluid.

Table 5 shows selected absolute performance information for circuitries optimized for each refrigerant. Overall, the high-pressure 'R410A group' shows higher capacities than the 'R22 group'. Within each group, R444B and R447A (zeotropic blends with the highest temperature glide) have the highest capacities because our simulations at the same dew-point temperature at the evaporator exit (7.2 °C) gave them the advantage of an increased mean effective temperature between the refrigerant and the air. For some zeotropes their two-phase glide was mitigated by the pressure drop. The outstanding performance of R717 was achieved on the strength of its thermophysical properties. The column with volumetric flow rate provides an indication on the compressor size required for individual refrigerants. Actual performance in a system will be also affected by the performance of the condenser and the overall system balance.

Table 5. Performance information for circuitries optimized for each refrigerant

(a) R22 alternative refrigerants

Refrigerant	Capacity (kW)	Mass flow rate ($kg \cdot h^{-1}$)	Pressure drop (kPa)	$T_{dew\text{-}point}$ drop due to pressure drop (K)	Two-phase temperature change[(1)] (K)	Volumetric flow rate[(2)] ($m^3 s^{-1}$)
R22	5.22	114.0	56.0	2.8	-2.8	$1.23 \cdot 10^{-3}$
MIX-1	6.07	149.6	36.4	2.1	1.9	$1.68 \cdot 10^{-3}$
R444B	6.96	124.2	33.7	1.9	6.0	$1.80 \cdot 10^{-3}$
R454C	6.56	159.3	40.7	2.3	3.8	$1.76 \cdot 10^{-3}$
R290	5.49	69.1	40.7	2.3	-2.3	$1.55 \cdot 10^{-3}$
R1270	5.67	68.7	43.8	2.1	-2.1	$1.30 \cdot 10^{-3}$
R717	6.32	20.3	17.3	0.8	-0.8	$1.30 \cdot 10^{-3}$

(b) R410A alternative refrigerants

Refrigerant	Capacity (kW)	Mass flow rate ($kg \cdot h^{-1}$)	Pressure drop (kPa)	$T_{dew\text{-}point}$ drop due to pressure drop (K)	Two-phase temperature change[(1)] (K)	Volumetric flow rate[(2)] ($m^3 s^{-1}$)
R410A	5.82	124.9	60.3	2.0	-1.9	$9.38 \cdot 10^{-4}$
MIX-2	6.12	106.6	55.6	2.0	-0.3	$1.06 \cdot 10^{-3}$
R32	6.00	85.1	35.4	1.1	-1.1	$8.83 \cdot 10^{-4}$
MIX-3	6.51	103.6	55.7	2.1	0.6	$1.15 \cdot 10^{-3}$
R452B	5.98	106.9	50.5	1.8	-0.8	$1.00 \cdot 10^{-3}$
R447A	6.69	112.4	67.1	2.6	1.2	$1.10 \cdot 10^{-3}$
R744	6.29	143.7	103.9	1.0	-1.0	$2.98 \cdot 10^{-3}$

[(1)] Isobaric two-phase temperature glide from inlet to outlet minus the drop of dew-point temperature, $T_{dew\text{-}point}$, due to pressure drop; [(2)] At the evaporator outlet

6. CONCLUDING REMARKS

We investigated the effect of an optimized refrigerant circuitry on the evaporator capacity for twelve R22 and R410A low-GWP alternative fluids. All fluids benefited from the optimization process carried out specifically for individual refrigerants. High-pressure refrigerants benefited most with R744 achieving a capacity increase of over 13 %, and all other achieving over 6 % improvement. Among lower-pressure refrigerants, capacity gains for R290, R1270, and R454C were over 5.5 %, and the capacity improvement for R717 was over 10 %. Smaller capacity improvements will be achieved in a complete system because of rebalancing of the system upon installation of a more effective evaporator. If optimized refrigerant circuitries were implemented in alternative refrigerant tests in existing equipment (hypothetical for ammonia and R744), these as-installed capacity improvements are estimated to be within 1 % to 4 %, and will be associated with 1 % to 2.5 % increases in the system COP over "drop-in" test results for the studied cases. Additional performance gains can be achieved through optimization of other components. The optimization results demonstrated that zeotropic blends with a significant temperature glide are particularly sensitive to the layout of refrigerant circuitry and may suffer significant performance degradation due to an improper circuitry design.

REFERENCES

Abdelaziz, O., Shrestha, S., Munk, J., Linkous, R., Goetzler, W., Guernsey, M., Kassuga, T., 2015. Alternative Refrigerant Evaluation for High-Ambient-Temperature Environments: R-22 and R-410A Alternatives for Mini-Split Air Conditioners, ORLL/TM-2015/536.

ASHRAE, 2013. ANSI/ASHRAE Standard 34-2013 Designation and Safety Classification of Refrigerants. ASHRAE, Atlanta.

Domanski, P.A., Yashar, D.A, Wojtusiak, J., 2014. EVAP-COND, Version 4.0: Simulation Models for Finned-Tube Heat Exchangers with Circuitry Optimization. National Institute of Standards and Technology, Gaithersburg, MD., http://www.nist.gov/el/building_environment/evapcond_software.cfm

Domanski, P. A., Yashar, D. A., 2007. Optimization of Finned-Tube Condensers Using an Intelligent System. Int. J. Refrig. 30 (3), 482-488.

Domanski, P.A., Yashar, D., 2006. Comparable Performance Evaluation of HC and HFC Refrigerants in an Optimized System, 7th IIR Gustav Lorentzen Conference on Natural Working Fluids, Trondheim, Norway.

Domanski, P.A., Yashar, D., Kim, M., 2005. Performance of a finned-tube evaporator optimized for different refrigerants and its effect on system efficiency, *Int. J. Refrig.*, 28 (6): 820-827.

Domanski, P.A., Yashar, D., Kaufman, KA., Michalski R.S., 2004. Optimized design of finned-tube evaporators using learnable evolution methods. *Int. J. HVAC&R Research*, 10(2): 201-212.

Domanski, P.A., 1989. Rating Procedure for Mixed Air Source Unitary Air Conditioners and Heat Pumps Operating in the Cooling Mode - Revision 1, NISTIR 89-4071, National Institute of Standards and Technology, Gaithersburg, MD

EU, 2014. Regulation No 517/2014 of the European Parliament and of the Council of 16 April 2014 on fluorinated greenhouse gases and repealing Regulation (EC) No 842/2006 (2014).

Lemmon, E.W., Huber, M.L., McLinden, M.O., 2013. NIST Standard Reference Database 23, NIST Reference Fluid Thermodynamic and Transport Properties—REFPROP, Version 9.1. Standard Reference Data Program, National Institute of Standards and Technology, Gaithersburg, MD.

Myhre, G., D. Shindell, F.-M. Bréon, W. Collins, J. Fuglestvedt, J. Huang, D. Koch, J.-F. Lamarque, D. Lee, B. Mendoza, T. Nakajima, A. Robock, G. Stephens, T. Takemura H. Zhang, 2013. Anthropogenic and Natural Radiative Forcing, Section 8 in: *Climate Change 2013: The Physical Science Basis, Fifth Assessment Report of the Intergovernmental Panel on Climate Change*. Cambridge, UK, Cambridge University Press.

Payne W. V., Domanski, P.A., 2003. Potential Benefits of Smart Refrigerant Distributors, report to Air-Conditioning and Refrigeration Technology Institute, report ARTI-21CR/605-200-50-01.

Yashar, D.A., Domanski, P.A., 2009. Particle Image Velocimetry Measurements and CFD-Based Predictions of Air Distribution at Evaporator Inlet and Outlet, NIST TN 1651, National Institute of Standards and Technology, Gaithersburg, MD.

Yashar, D.A., Domanski, P.A., Lee, S., 2010. Evaporator Optimization for Non-Uniform Air Distribution. Proceedings of Conference of Sustainable Refrigeration and Heat Pump Technology, Stockholm, Sweden.

Yashar, D.A., Lee, S., Domanski, P.A., 2015. Rooftop Air-Conditioning Unit Performance Improvement Using Refrigerant Circuitry Optimization, Applied Thermal Engineering, 83:81-87.